

**SYNTHESES, STRUCTURES AND PHYSICAL PROPERTIES OF CYANIDE-BRIDGED  
M(II)-Ni(II) BIMETALLIC COMPLEXES WITH 2-PYRIDINEETHANOL  
(M(II) = Fe, Co and Ni)**

**Elvan SAYIN<sup>1,\*</sup> Güneş Süheyla KÜRKÇÜOĞLU<sup>2</sup>**

<sup>1</sup>Department of Physics, Graduate School of Natural and Applied Sciences, Eskişehir Osmangazi University,  
26480 Eskişehir, Turkey

<sup>2</sup>Department of Physics, Faculty of Arts and Sciences, Eskişehir Osmangazi University,  
26480 Eskişehir, Turkey.

**ABSTRACT**

In this study, cyanide complexes with chemical formula  $[M(\text{hepH})_2\text{Ni}(\mu\text{-CN})_2(\text{CN})_2]$  (hepH = 2-pyridineethanol; M = Fe(II), Co(II) and Ni(II); abbreviated to hereafter **M-hepH-Ni**) were obtained for the first time. The structures of these complexes were determined by using FT-IR and Raman spectroscopies, thermal and elemental analyses. The electrical and magnetic properties of the complexes were investigated by four-probe and Evans methods, respectively. Vibration assignments are obtained for all the observed bands and the spectral feature has been shown supported to the structure of complexes. Thermal behaviors of these complexes were examined using TG, DTG and DTA curves in the temperature range 30-700 °C in the static air atmosphere. According to thermal analysis curves, it has seen that neutral ligands (hepH) are released and cyanide ligands are decomposed in the complexes, followed usual decomposition mechanism. The final decomposition products are found to be the corresponding metal oxides. The magnetic measurements of the complexes are compared with experimental and theoretical values of the magnetic moment. Furthermore, **Fe-hepH-Ni**, **Co-hepH-Ni** and **Ni-hepH-Ni** complexes are determined to be paramagnetic.

**Keywords:** FT-IR and Raman spectra, Tetracyanonickelate(II) complex, 2-Pyridineethanol, Cyanide bridged complex, Electrical conductivity

**2-PİRİDİNİETANOL İLE SİYANÜR-KÖPRÜLÜ M(II)-Ni(II) İKİ METALLİ  
KOMPLEKSLERİN SENTEZİ, YAPISI VE FİZİKSEL ÖZELLİKLERİ  
(M(II) = Fe, Co ve Ni)**

**ÖZET**

Bu çalışmada  $[ML_2\text{Ni}(\mu\text{-CN})_2(\text{CN})_2]$  (L= 2-piridinetanol (hepH); M = Fe(II), Co(II) veya Ni(II); bundan sonra **M-hepH-Ni** olarak kısaltılmıştır.) formülü ile verilen siyanür kompleksleri ilk kez elde edilmiştir. Bu komplekslerin yapıları kırmızı-altı ve Raman spektroskopisi, termal ve elementel analiz teknikleri kullanılarak belirlenmiştir. Komplekslerin elektriksel özellikleri dört uç metodu, manyetik özellikleri ise Evans metodu kullanılarak araştırılmıştır. Titreşim işaretlemeleri tüm gözlenen bandlar için elde edilmiş ve spektral özelliklerin komplekslerin yapılarını destekledikleri görülmüştür. Komplekslerin termal davranışları kuru havada 30 - 700 °C sıcaklık aralığında TG, DTG ve DTA eğrileri kullanılarak incelenmiştir. Termal analiz eğrilerine göre, hepH ligandının ve siyanür grubunun yapılardan uzaklaşmaları görülmüştür. Son bozunma ürünlerinin metal oksitler olduğu bulunmuştur. Manyetik ölçümlerde komplekslerin deneysel ve teorik manyetik moment değerleri karşılaştırılmıştır. Ayrıca, **Fe-hepH-Ni**, **Co-hepH-Ni** ve **Ni-hepH-Ni** komplekslerinin paramanyetik oldukları belirlenmiştir.

**Anahtar Kelimeler:** FT-IR ve Raman spektrumları, Tetrasiyanonikelat(II) kompleksi, 2-Piridinetanol, Siyanür köprülü kompleks, Elektriksel iletkenlik

**1. INTRODUCTION**

A large number of metal complexes have been extensively synthesized in this half century, focusing on homo- or heteronuclear metal complexes [1, 2]. On the other hand, polynuclear complexes are expected to provide a variety of physical and chemical properties such as magnetism [3-5], electric

\* Corresponding Author: [elvansayin@hotmail.com](mailto:elvansayin@hotmail.com)

conductivity [6], homo- and hetero-geneous catalysts [7]. Polynuclear complexes are the compounds containing multifunctional ligands with electronic structures which provide unique electronic properties.

In terms of physical incorporating transition metals, firstly, the metals such as Mn, Fe, Co can use them as building blocks to direct a certain framework topology and secondly, they can be chosen based on their electronic functionality, such as for magnetism or redox potential. A number of transition metals exist in more than one oxidation state, i.e. Mn(II)/(III), Fe(II)/(III) and Co(II)/(III), so that an even larger range of options exist. Characteristic coordination geometries that are seen in transition metals in coordinations polymers include linear, bent, trigonal, square-planar, tetragonal, prismatic and octahedral [4, 8-10]. Thus, transition metals can be used as building blocks ranging from 2- to 6-binding.

Short bridging pseudohalide ligands such as cyanides, azides and nitrile donors provide a convenient way of connecting transition metals in the solid state. The cyanide group, itself, is also a good ligand for transition metals [4]. When cyanide ligand comes into connected with dissolved metal ions, metal-cyanide complexes are formed. Cyanide complexes are metal-ligand complexes that extend “infinitely” into one, two or three dimensions (1D, 2D or 3D, respectively) with covalent metal-ligand bonding. An interesting feature of the cyanide ligand is its ability to act either as a terminal or as a bridging ligand. The cyanide group has a strong electron-withdrawing character, as well as the talent to the metal [11].

In our previous studies, we have reported the tetracyanonickelate(II), tetracyanopalladate(II) and tetracyanoplatinate(II) complexes with hepH [12-14]. As a part of our continuing research on cyanide complexes, herein we described the syntheses and characterizations of tetracyanonickelate(II) complexes with different metals such as Fe(II), Co(II) and Ni(II). We characterized the structures of these complexes by FT-IR and Raman spectroscopies, elemental and thermal analyses. Also, we determined electrical conductivity and magnetic susceptibilities of the all complexes.

## **2. EXPERIMENTAL SECTION**

### **2.1. Materials and Instrumentation**

Iron(II) chloride tetrahydrate ( $\text{FeCl}_2 \cdot 4\text{H}_2\text{O}$ , 99%), cobalt(II) chloride ( $\text{CoCl}_2$ , 99%), nickel(II) chloride hexahydrate ( $\text{NiCl}_2 \cdot 6\text{H}_2\text{O}$ , 97%), potassium cyanide (KCN, 96%) and 2-pyridineethanol ( $\text{C}_7\text{H}_9\text{NO}$ , 98%) were purchased from commercial sources and used without further purification. Elemental analyses were carried out on a LECO, CHNS-932 analyzer for C, H and N at the Middle East Technical University, Central Laboratory. The FT-IR spectra were recorded as pure solids by ATR (Attenuated Total Reflection) in the range of  $4000\text{-}225\text{ cm}^{-1}$  with a  $4\text{ cm}^{-1}$  spectral resolution by using a Perkin Elmer 100 FT-IR spectrometer, which was calibrated by means of polystyrene and  $\text{CO}_2$  bands. The Raman spectra were recorded in the range of  $4000\text{-}225\text{ cm}^{-1}$  on a Bruker Senterra Dispersive Raman instrument using 785 nm laser excitation. A Perkin Elmer Diamond TG/DTA thermal analyzer was used to record simultaneous TG, DTG and DTA curves in a static air atmosphere at a heating rate of  $10\text{ K min}^{-1}$  in the temperature range of  $30\text{-}700\text{ }^\circ\text{C}$  using platinum crucibles. The electrical conductivity measurements were carried out on the complexes using the four-probe method at the room temperature with the programmable dc current source (Keithley 2601 A System Sourcemeter). Magnetic Susceptibilities at room temperature were measured by the Evans method, a Sherwood Scientific MXI model Gouy magnetic balance.

## 2.2 Preparation of the Complexes

### 2.2.1. $M[Ni(CN)_4] \cdot H_2O$ (M = Fe, Co or Ni)

To water solution of  $NiCl_2 \cdot 6H_2O$  (0.238 g, 1 mmol) was added a solution of KCN (0.260 g, 4 mmol) in water (10 mL) and yellow  $K_2[Ni(CN)_4] \cdot H_2O$  was crystallized.  $K_2[Ni(CN)_4] \cdot H_2O$  (0.259 g, 1 mmol) to which was added metal chloride solutions ( $FeCl_2 \cdot 4H_2O = 0.199$  g,  $CoCl_2 = 0.129$  g or  $NiCl_2 \cdot 6H_2O = 0.260$  g, 1 mmol) became  $M[Ni(CN)_4] \cdot H_2O$ . The colors of  $Fe[Ni(CN)_4] \cdot H_2O$ ,  $Co[Ni(CN)_4] \cdot H_2O$  and  $Ni[Ni(CN)_4] \cdot H_2O$  are brown, pink and pale blue (Table 1), respectively.

### 2.2.2. $[M(hepH)_2Ni(\mu-CN)_2(CN)_2]$ (M = Fe, Co or Ni)

A mixture of  $Fe[Ni(CN)_4] \cdot H_2O$  (0.243 g, 1 mmol) in water (10 mL) and hepH (0.246 g, 2 mmol) in ethanol (10 mL) was stirred at 55 °C for 4 h in a temperature-controlled bath. The obtained solution were filtered, washed with ethanol and ether, respectively and dried in a desiccator above  $P_2O_5$ .

**Co-hepH-Ni** and **Ni-hepH-Ni** complexes were obtained in a similar method to **Fe-hepH-Ni**, but Fe(II) was replaced by Co(II) (0.240 g) and Ni(II) (0.240 g).

## 3. RESULTS AND DISCUSSION

### 3.1. Elemental Analyses

The analytical data, elemental analyses (C, H and N), molar ratio and color of the **M(II)-hepH-Ni** (M(II) = Fe, Co and Ni) complexes are shown in Table 1. The resulting elemental analysis values are in good agreement with the calculated values. Based on the obtained data, the prepared complexes are formulated as  $[M(hepH)_2Ni(\mu-CN)_2(CN)_2]$  (M(II)= Fe, Co and Ni). The formation of 1:2 complexes is strongly supported by elemental and thermal analyses. **Fe-hepH-Ni**, **Co-hepH-Ni** and **Ni-hepH-Ni** complexes have a brown, pink and pale blue color, respectively.

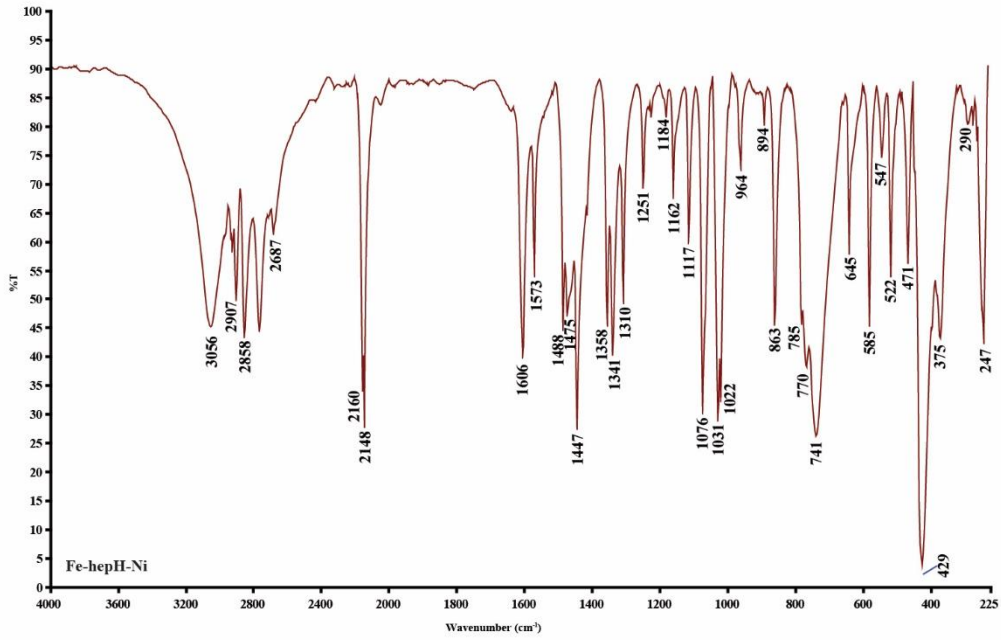
**Table 1.** Analytical and physical data of the complexes.

Complex	Molecular formula	$M_{\text{wt}}$ (g/mol)	Elemental analyses						$\mu$		Color
			C%		H%		N%		Calc.	Found	
			Calc.	Found	Calc.	Found	Calc.	Found			
$[Fe(hepH)_2Ni(\mu-CN)_2(CN)_2]$	$C_{18}H_{18}N_6O_2NiFe$	464.91	46.50	45.96	3.90	3.88	18.08	18.15	4.89	4.73	Brown
$[Co(hepH)_2Ni(\mu-CN)_2(CN)_2]$	$C_{18}H_{18}N_6O_2NiCo$	468.00	46.19	45.85	3.88	3.75	17.96	17.79	3.87	3.61	Pink
$[Ni(hepH)_2Ni(\mu-CN)_2(CN)_2]$	$C_{18}H_{18}N_6O_2Ni_2$	467.76	46.22	45.98	3.88	3.96	17.97	18.01	2.83	2.92	Pale Blue

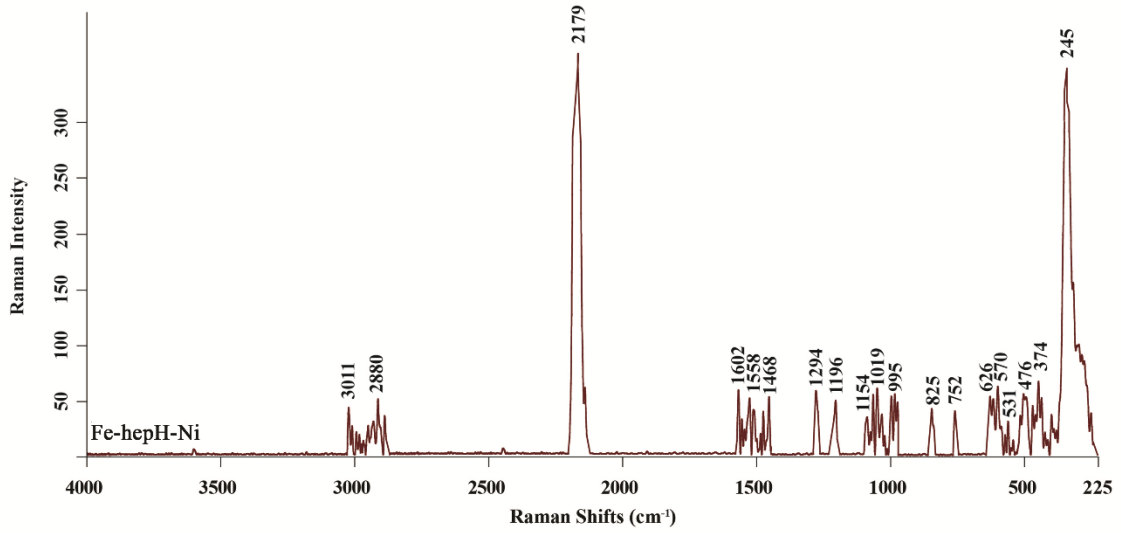
### 3.2. Vibrational Spectra

#### 3.2.1. Vibrational (FT-IR and Raman) spectra of the complexes

The FT-IR and Raman spectra of the **M(II)-hepH-Ni** (M(II) = Fe, Co and Ni) complexes have been recorded at room temperature (Figures 1-3). The vibration assignments of the observed bands are listed in Table 2. In the FT-IR and Raman spectra of **M(II)-hepH-Ni** (M(II) = Fe, Co and Ni) complexes, the most bands are observed belong to organic motif modes. The values of wavenumbers are collected in Table 2, together with the assignment of characteristic bands [14].

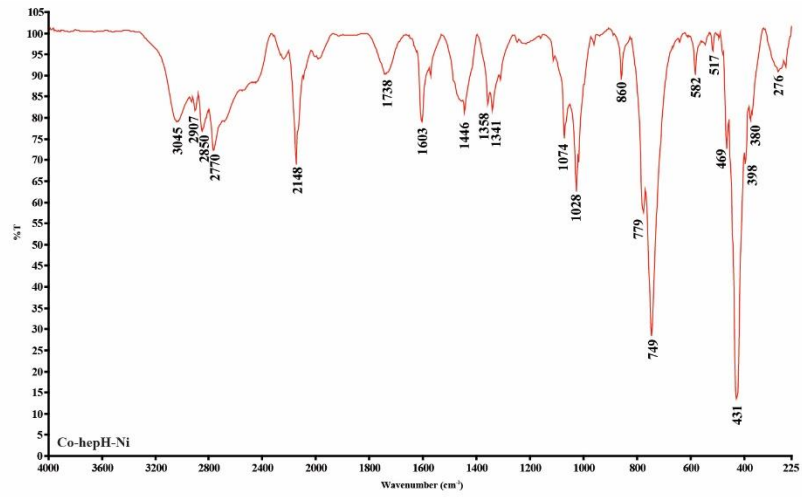


(a)

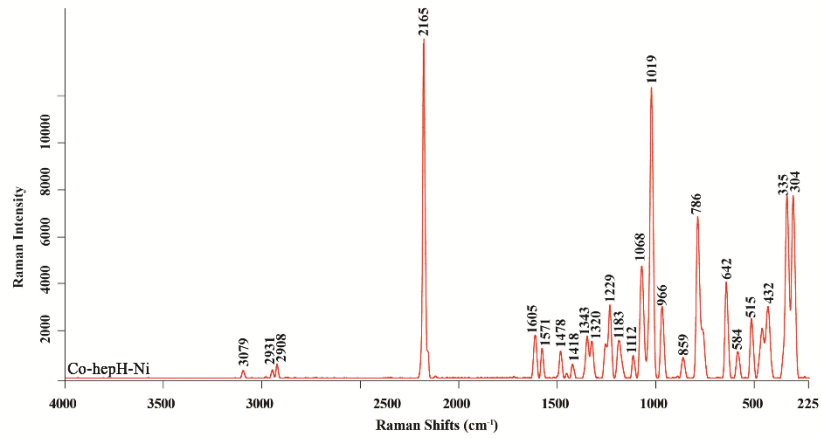


(b)

**Figure 1.** The FT-IR (a) and Raman (b) spectra of **Fe-hepH-Ni** complex



(a)



(b)

**Figure 2.** The FT-IR (a) and Raman (b) spectra of Co-hepH-Ni complex

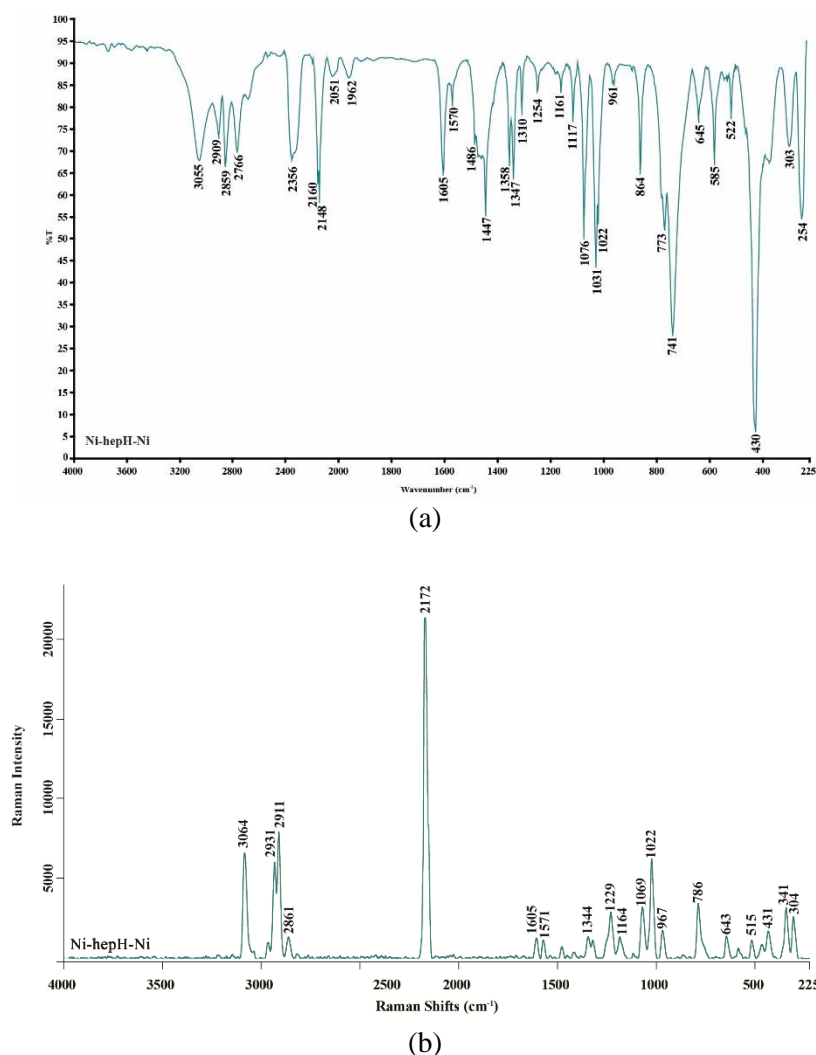


**Figure 3.** The FT-IR (a) and Raman (b) spectra of Ni-hepH-Ni complex

The -OH group in a molecule can be identified on the basis of three vibrations namely stretching, in-plane bending and out of plane bending vibrations. Experimental FT-IR spectrum gives a broad curve from 3382 to 3246  $\text{cm}^{-1}$  with strong intensity for  $\nu(\text{OH})$  stretching frequency [15]. The occurrence of this band confirms that the molecules are binding through the intermolecular hydrogen bonds. The observed band due to  $\nu(\text{OH})$  is very broad in the case of free hepH molecules, which indicates the intermolecular hydrogen bonding between the  $-\text{CH}_2\text{OH}$  groups. In the complexes, weak bands appear at 3102  $\text{cm}^{-1}$  in **Fe-hepH-Ni**, 3121  $\text{cm}^{-1}$  in **Co-hepH-Ni** and 3167  $\text{cm}^{-1}$  in **Ni-hepH-Ni** due to  $\nu(\text{OH})$ .

The shift to lower wavenumbers of these stretching bands may be attributed to covalent bondings in the complexes. The  $\delta(\text{OH})$  deformation vibrations give rise to a medium to strong band in the region 1250-1117  $\text{cm}^{-1}$  and is not affected due to hydrogen bonding unlike stretching and out-of-plane bending wavenumbers [16]. These bands are shown at Table 2. The substituted aromatic structure shows the presence of  $\nu(\text{CH})$  stretching vibrations in the region 3100-3000  $\text{cm}^{-1}$  and this is the characteristic region for the identification of the  $\nu(\text{CH})$  stretching bands [17, 18]. Hence, asymmetric  $\nu(\text{CH})$  stretching bands of free hepH molecule in the FT-IR and Raman spectra have been assigned at 3087 and 3071  $\text{cm}^{-1}$ , respectively. In the complexes, the asymmetric and symmetric  $\nu(\text{CH})$  bands are expected in the region 2940 - 2915  $\text{cm}^{-1}$  and 2870 - 2840  $\text{cm}^{-1}$ , respectively [19].

In the all complexes,  $\nu(\text{CH})$  asymmetric stretching bands were assigned in the region of 2931 - 2907  $\text{cm}^{-1}$  in FT-IR spectra. These bands were observed in the region of 2967-2958  $\text{cm}^{-1}$  in Raman spectra of the complexes. In the complexes, the symmetric  $\nu(\text{CH})$  stretching vibrations are observed in the regions of 2909 - 2852  $\text{cm}^{-1}$  (in the FT-IR spectra) and 2922 - 2855  $\text{cm}^{-1}$  (in the Raman spectra). Also, the  $\delta_{\text{ring}}(\text{CH})$  deformation bands arising from  $-\text{CH}_2$  group in all complexes are observed in the frequency range of 1508 - 1446  $\text{cm}^{-1}$  in the FT-IR spectra. The  $\nu(\text{CC})$  bands of the pyridine ring were appeared in the spectral range of 1650 - 1200  $\text{cm}^{-1}$  [20]. The  $\nu_{\text{ring}}(\text{CC})$  stretching bands are appeared at 1606 and 1573  $\text{cm}^{-1}$  for **Fe-hepH-Ni**, 1605 and 1571  $\text{cm}^{-1}$  for **Co-hepH-Ni**, 1605 and 1573  $\text{cm}^{-1}$  for **Ni-hepH-Ni** in the FT-IR spectra. The same bands are observed at 1601 and 1579  $\text{cm}^{-1}$  for **Fe-hepH-Ni**, 1606 and 1572  $\text{cm}^{-1}$  for **Co-hepH-Ni**, 1605 and 1571  $\text{cm}^{-1}$  for **Ni-hepH-Ni** in the Raman spectra. The  $\delta(\text{CH})$  vibrations are observed in the regions of 1350 - 950  $\text{cm}^{-1}$  and 950 - 600  $\text{cm}^{-1}$ , respectively [21]. The  $\nu(\text{CN})$  stretching vibration band is observed as medium intensity band at 1278  $\text{cm}^{-1}$  in FT-IR and this band not observed in Raman spectrum. This band is mixed with  $\delta(\text{CH})$ . The similar vibration bands in the FT-IR spectra of the complexes are observed at 1274 and 1251  $\text{cm}^{-1}$  in **Fe-hepH-Ni**, 1273 and 1250  $\text{cm}^{-1}$  in **Co-hepH-Ni**, 1279 and 1250  $\text{cm}^{-1}$  in **Ni-hepH-Ni**, respectively.

The FT-IR spectra at the low frequency region of the isolated solid complexes showed a group of new bands with different intensities which characteristics for  $\nu(\text{M-N})$ . In the low wavenumber region, the  $\nu(\text{M-N})$  and  $\delta(\text{N-M-N})$  vibration bands provide the information about the structure of the metal-ligand. In the octahedral metal-hexammine complexes, these vibrational bands are expected to appear in the range of 570 - 240  $\text{cm}^{-1}$  and 340 - 90  $\text{cm}^{-1}$  [22]. The  $\nu(\text{M-N})$  vibration bands were observed at 547 and 468  $\text{cm}^{-1}$  for **Fe-hepH-Ni**, 548 and 469  $\text{cm}^{-1}$  for **Co-hepH-Ni**, 547 and 471  $\text{cm}^{-1}$  for **Ni-hepH-Ni**. The  $\delta(\text{N-M-N})$  bands observed at 237  $\text{cm}^{-1}$  for **Fe-hepH-Ni**, 237  $\text{cm}^{-1}$  for **Co-hepH-Ni**, 235  $\text{cm}^{-1}$  for **Ni-hepH-Ni**. The  $\nu(\text{M-O})$  band observed at 327  $\text{cm}^{-1}$  for **Fe-hepH-Ni**, 329  $\text{cm}^{-1}$  for **Co-hepH-Ni** and at 330  $\text{cm}^{-1}$  for **Ni-hepH-Ni**. These  $\nu(\text{M-N})$  and  $\nu(\text{M-O})$  stretching bands are similar to the corresponding values found and reported in  $[\text{M}(\text{OHepy})_2\text{Ni}(\text{CN})_4]_n$  ( $\text{M}(\text{II}) = \text{Cu}, \text{Zn}$  and  $\text{Cd}$ ) [14].

### 3.2.2. $[\text{Ni}(\text{CN})_4]^{2-}$ group vibrations

The  $\nu(\text{CN})$  stretching vibrations are the most characteristic bands in the cyanide groups resulting sharp and strong bands which may easily be determined in the range of 2200-2000  $\text{cm}^{-1}$  [22]. The vibrational wavenumbers for  $[\text{Ni}(\text{CN})_4]^{2-}$  group in  $\text{K}_2[\text{Ni}(\text{CN})_4] \cdot \text{H}_2\text{O}$  and in complexes are presented in Table 3. The bands of the  $[\text{Ni}(\text{CN})_4]^{2-}$  in the complexes are assigned on the basis of the work of Mc Cullough et al., who presented vibrational data for the  $[\text{Ni}(\text{CN})_4]^{2-}$  in  $\text{Na}_2[\text{Ni}(\text{CN})_4]$  [23]. The  $\nu(\text{CN})$  frequency shifts towards higher frequencies due to formation of the cyanide-bridge. The FT-IR spectrum of the mononuclear compound  $\text{K}_2[\text{Ni}(\text{CN})_4]$  showed a band at 2122  $\text{cm}^{-1}$ . This position was observed at 2080  $\text{cm}^{-1}$  in ionic KCN as a single absorption band, which can be assigned to the  $\nu(\text{CN})$  [24]. Two strong and sharp absorption bands are observed in the FT-IR spectra of the complexes. This case is given as following; at 2160 and 2148  $\text{cm}^{-1}$  for **Fe-hepH-Ni**, at 2153 and 2148  $\text{cm}^{-1}$  for **Co-hepH-Ni**, at 2160 and 2148  $\text{cm}^{-1}$  for **Ni-hepH-Ni** can easily be attributed to bridging cyanide and terminal cyanide bands, respectively. The  $[\text{Ni}(\text{CN})_4]^{2-}$  group vibrations in the complexes are found at higher wavenumber than in  $\text{K}_2[\text{Ni}(\text{CN})_4] \cdot \text{H}_2\text{O}$  salt. This is explained as the mechanical coupling of the internal modes of  $[\text{Ni}(\text{CN})_4]^{2-}$  with the M-NC vibrations. In some studies, this was discussed the electronic effects on the stretching frequencies in both bridging and terminal cyanide ligands [25]. The  $[\text{Ni}(\text{CN})_4]^{2-}$  anion possesses ideally  $D_{4h}$  symmetry and, thus, will have 16 fundamental vibrations ( $2A_{1g}, 1A_{2g}, 2B_{1g}, 2B_{2g}, 1E_g, 2A_{2u}, 2B_{2u},$  and  $4E_u$ ) [24, 26]. According to these results,  $A_{2u}$  and  $E_u$  are infrared active, while  $A_{1g}, B_{1g}, B_{2g},$  and  $E_g$  are Raman active. The  $A_{2g}$  and  $B_{2u}$  vibrations are inactive. The  $A_{1g}$  and  $B_{1g}$  cyanide stretching modes are observed in 2179 and 2169  $\text{cm}^{-1}$  in **Fe-hepH-Ni**, 2165 and 2157  $\text{cm}^{-1}$  in **Co-hepH-Ni**, 2172 and 2132  $\text{cm}^{-1}$  in **Ni-hepH-Ni** in the Raman spectra of the complexes. In the low frequency region of the FT-IR spectra,  $\nu(\text{Ni-CN})$  stretching and  $\delta(\text{Ni-CN})$  bending vibration bands in the 600–400  $\text{cm}^{-1}$  are observed for the complexes. The bands observed at 471 and 429  $\text{cm}^{-1}$  in **Fe-hepH-Ni**, 469 and 430  $\text{cm}^{-1}$  in **Co-hepH-Ni** 471 and 430  $\text{cm}^{-1}$  in **Ni-hepH-Ni**

in the FT-IR spectra of the complexes might be attributed to the  $\nu(\text{Ni-CN})$  stretching vibrations and  $\delta(\text{Ni-CN})$  bending vibrations, respectively.

**Table 2.** The FT-IR and Raman wavenumbers of the hepH and the complexes ( $\text{cm}^{-1}$ )

No	Assignments (PED%) [14]	hepH		Fe-hepH-Ni		Co-hepH-Ni		Ni-hepH-Ni	
		Experimental (liquid)		FT-IR	Raman	FT-IR	Raman	FT-IR	Raman
		FT-IR	Raman						
1	$\nu(\text{OH})$ (100)	3382 m	-	3102 vw	-	3121 vw	-	3167 vw	-
2	$\nu(\text{CH})$ (90)	3087 vw	3075 vw	3067 w	3090 w	3061 w	3079 m	3065 w	3064 m
3	$\nu(\text{CH})$ (99)	3071 vw	-	3056 w	3048 vw	3045 vw	3042 vw	3055 w	3036 vw
4	$\nu(\text{CH})$ (91)	-	-	-	-	-	-	-	-
5	$\nu(\text{CH})$ (94)	3013 m	3024 vw	2969 w	3014 w	2966 w	3018 w	2972 w	3005 w
6	$\nu_{\text{as}}(\text{CH}_2)+\nu_{\text{as}}(\text{CH}_2)$ (99)	2954 m	3008 vw	2949 w	-	2950 vw	-	2955 w	-
7	$\nu_{\text{as}}(\text{CH}_2)+\nu_{\text{as}}(\text{CH}_2)$ (87)	2929 m	2925 vw	2928 w	2958 vw	2931 w	2960 vw	2925 w	2967 vw
8	$\nu_{\text{as}}(\text{CH})+\nu_s(\text{CH}_2)$ (93)	2904 vw	-	2907 w	2920 w	2908 w	2922 vw	2909 w	2911 m
9	$\nu_s(\text{CH}_2)+\nu_s(\text{CH}_2)$ (94)	2870 m	-	2858 m	2855 w	2852 m	2858 w	2859 m	2861 vw
10	$\nu_{\text{ring}}(\text{C-C})$ (54)	1593 s	1582 m	1606 m	1601 vw	1605 m	1606 m	1605 m	1605 vw
11	$\nu_{\text{ring}}(\text{C-C})$ (52)	1569 m	1554 w	1573 m	1579 vw	1571 m	1572 w	1573 m	1571 vw
12	$\delta_{\text{ring}}(\text{CH}_2)$ (72)	1506 vw	-	1508 vw	1559 vw	1506 vw	1552 vw	1507 vw	1559 vw
13	$\delta(\text{CH})$ (16)+ $\nu(\text{NC})$ (19)+ $\delta(\text{HCN})$ (33)	1476 s	1460 sh	1488 m	1488 w	1486 m	1478 vw	1487 m	1482 vw
14	$\delta(\text{CH}_2)$ (75)	1435 s	-	1447 m	1468 w	1446 m	1478 w	1447 m	1479 w
15	$\delta(\text{CCH})$ (51)	1417 sh	-	1418 vw	1431 vw	1418 vw	1434 vw	1417 vw	1437 vw
16	$\delta(\text{COH})$ (13)+ $\delta(\text{CH}_2)$ (19)+ $\nu(\text{CCCH})$ (41)	1370 m	1392 vs	1358 m	1380 m	1358 m	1379 w	1358 m	1379 w
17	$\delta(\text{COH})$ (19)+ $\delta(\text{CH}_2)$ (34)+ $\nu(\text{CCCH})$ (10)	1337 sh	1320 sh	1341 m	1357 w	1342 m	1344 w	1342 m	1344 vw
18	$\delta(\text{CCH})$ (33)+ $\delta(\text{HCN})$ (26)	1316 vw	1295 sh	1310 m	1307 w	1311 m	1306 w	1310 m	1304 w
19	$\delta(\text{COH})$ (20)+ $\nu(\text{CCCH})$ (29)	1301 w	-	1283 vw	-	1281 vw	-	1285 vw	-
20	$\nu(\text{NC})$ (29)+ $\delta(\text{HCN})$ (12)+ $\delta(\text{CCH})$ (15)	1278 m	-	1274 vw	1281 vw	1273 vw	1278 vw	1279 vw	1278 vw
21	$\nu(\text{NC})$ (39)+ $\nu(\text{CCCH})$ (10)	1241 m	1234 m	1251 w	1257 w	1250 w	1256 w	1250 w	1252 m
22	$\delta(\text{CC})$ (24)+ $\delta(\text{CCH})$ (12)+ $\delta(\text{CNC})$ (10)	1223 w	-	1228 w	1224 m	1228 vw	1229 w	1228 vw	1229 vw
23	$\nu(\text{CC})$ (11)+ $\delta(\text{CCH})$ (74)	1150 m	1193 vw	1162 w	1187 m	1162 w	1183 w	1163 w	1183 m
24	$\delta(\text{COH})$ (16)+ $\delta(\text{CCH})$ (20)	1099 m	1113 w	1117 m	1167 m	1114 m	1165 vw	1117 m	1164 vw
25	$\nu(\text{CC})$ (12)+ $\delta(\text{CCH})$ (21)	-	-	1076 s	1072 m	1074 s	1068 m	1076 s	1069 vw
26	$\nu(\text{CC})$ (49)	1048 s	1065 s	1031 s	1031 w	1028 s	1020 m	1031 s	1022 m
27	$\nu(\text{OC})$ (87)	1002 s	1011 s	1022 m	1020 m	1020 m	1019 m	1022 m	1022 m
28	$\nu(\text{CC})$ (49)	993 sh	-	998 w	996 m	998 w	1000 vw	998 w	997 vw
29	$\nu(\text{CC})$ (38) + $\delta(\text{HCO})$ (10)	-	-	-	979 w	-	975 w	-	970 w
30	$\nu(\text{CCCH})$ (48)+ $\nu(\text{HCCN})$ (17)+ $\nu(\text{CCCC})$ (12)	966 vw	971 vw	964 w	965 w	970 sh	966 w	968 w	967 vw
31	$\nu(\text{CN})$ (10)+ $\nu(\text{CC})$ (11)+ $\delta(\text{CCH})$ (25)	952 w	968 vw	953 sh	946 w	962 vw	953 vw	959 sh	954 vw
32	$\nu(\text{HCCC})$ (13)+ $\nu(\text{HCCN})$ (54)+ $\nu(\text{CCCN})$ (14)	940 sh	925 vw	943 vw	937 vw	941 vw	931 vw	947 vw	937 m
33	$\nu(\text{HCCC})$ (48)+ $\nu(\text{HCCN})$ (24)	890 m	852 w	894 w	891 vw	892 w	887 vw	894 w	890 vw
34	$\nu(\text{CC})$ (22)+ $\delta(\text{NCC})$ (11)+ $\delta(\text{CCC})$ (23)	862 m	822 vw	863 m	852 vw	861 m	859 vw	864 m	856 vw
35	$\nu(\text{HCCC})$ (47)	781 sh	793 m	785 w	786 w	784 m	786 m	784 m	786 w
36	$\nu(\text{HCCC})$ (13)+ $\nu(\text{HCCN})$ (30)+ $\nu(\text{CCCC})$ (12)+ $\nu(\text{CCCN})$ (11)+ $\nu(\text{CNCC})$ (19)	750 vs	765 sh	741 s	739 w	749 s	741 w	741 s	748 w
37	$\delta(\text{CCC})$ (17)+ $\delta(\text{NCC})$ (32)+ $\delta(\text{CCN})$ (17)	728 sh	645 m	692 sh	664 w	694 sh	666 w	695 vw	645 vw
38	$\delta(\text{CCC})$ (17)+ $\delta(\text{NCC})$ (32)+ $\delta(\text{CNC})$ (17)	632 m	623 sh	645 vw	644 w	643 vw	642 w	645 w	643 vw
39	$\delta(\text{CCC})$ (24)+ $\delta(\text{CNC})$ (15)	585 s	588 m	585 m	570 m	585 m	584 w	585 m	585 w
40	$\nu(\text{HCCC})$ (13)+ $\nu(\text{CNCC})$ (35)	505 m	477 vw	507 w	523 w	504 w	515 w	503 vw	515 vw
41	$\nu(\text{HCCC})$ (18)	403 m	417 vw	399 vw	398 sh	398 vw	397 vw	396 vw	394 vw
42	$\delta(\text{CCN})$ (55)	357 m	350 sh	352 w	350 m	359 w	338 w	351 w	341 w
43	$\nu(\text{CC})$ (15)+ $\nu(\text{HOCC})$ (15)+ $\delta(\text{OCC})$ (32)	336 sh	335 vw	331 vw	319 m	328 vw	-	-	313 vw
44	$\nu(\text{HOCC})$ (76)	285 m	283 m	290 vw	285 vw	288 vw	280 vw	-	275 vw
45	$\delta(\text{CCC})$ (23)+ $\nu(\text{CCCC})$ (14)	254 m	-	253 w	245 s	256 vw	253 vw	254 m	244 vw
46	$\delta_s(\text{CH}_2)$	-	-	-	-	-	-	-	-
47	$\delta_s(\text{CH}_2)$	-	-	-	-	-	-	-	-
48	$\delta_s(\text{skeletal})$	-	-	-	-	-	-	-	-

Abbreviations used:  $\nu$ , stretching;  $\delta$ , bending; t, torsion; r, ring; s, strong; m, medium; w, weak; sh, shoulder; v, very

**Table 3.** Vibrational wavenumbers of the polymeric sheet and metal-ligand vibrations in the complexes (cm<sup>-1</sup>)

Assignments	K <sub>2</sub> [Ni(CN) <sub>4</sub> ]·H <sub>2</sub> O [23,27]	Fe-hepH-Ni	Co-hepH-Ni	Ni-hepH-Ni
A <sub>1g</sub> , ν(C≡N)	(2160) vs	(2179) vs	(2165) vs	(2172) vs
B <sub>1g</sub> , ν(C≡N)	(2137) m	(2169) m	(2157) m	(2132) m
E <sub>u</sub> , ν(C≡N)	2122 vs	2160 s, 2148 vs	2153 s, 2148 vs	2160 s, 2148 vs
ν( <sup>13</sup> CN)	2084 w	2084 vw	2084 vw	2085 vw
E <sub>u</sub> , ν(Ni-C)	540 w	547 w	548 vw	546 w
A <sub>2u</sub> , π(Ni-CN)	443 w	471 s	469 m	471 m
E <sub>u</sub> , δ(Ni-CN)	417 s	429 vs	431 vs	430 vs
A <sub>1g</sub> , ν(Ni-C)	(374)	(380) w	(379) w	379 vw
E <sub>g</sub> , π(Ni-CN)	298	296 vw	290 vw	303 vw
B <sub>2g</sub> , δ(C-Ni-C)	109	-	-	-
<b>Metal-ligand vibrations [28]</b>				
A <sub>2u</sub> , ν(M-N) <sub>(hepH)</sub>	-	380 m	372 vw	378 w
E <sub>u</sub> , ν(M-N) <sub>(CN)<sub>4</sub></sub>	-	278 w	277 w	278 vw
A <sub>1g</sub> /E <sub>g</sub> , ν(M-N) <sub>(hepH)</sub>	-	274 w	272 w	273 w
A <sub>2u</sub> , δ(N-M-N) <sub>(hepH)</sub>	-	237 m	237 w	235 vw
E <sub>u</sub> , δ(N-M-N) <sub>(CN)<sub>4</sub></sub>	-	230 w	228 w	226 w

Abbreviations used; s strong, m medium, w weak, sh shoulder, v very. The symbols ν, δ and π refer to valence, in-plane and out-of-plane vibrations, respectively. Raman bands are given in parentheses.

### 3.3. Thermal Behaviors of the Complexes

Thermal and elemental analyses of the complexes are also considered besides to the vibrational spectroscopic studies that in turn ensure the structural information on the complexes. The thermal analyses are performed by TG, DTA and TGA methods in the temperature range of 30-700 °C, the thermal analysis curves for **Fe-hepH-Ni**, **Co-hepH-Ni** and **Ni-hepH-Ni** are given in Figures 4a-c.

The thermal analysis curves for the **Fe-hepH-Ni** and **Ni-hepH-Ni** complexes are similar and decomposition takes place in one stage. The stages of the **Fe-hepH-Ni** and **Ni-hepH-Ni** is related with two hepH ligands and -CN groups in the temperature range of 74-382 °C for **Fe-hepH-Ni** and 37-372 °C for **Ni-hepH-Ni** [found (calcd.): 71.46% (75.36%) in **Fe-hepH-Ni** and 71.12% (74.90%) in **Ni-hepH-Ni**]. The complexes begin to decompose with endothermic and exothermic peaks. A strong exothermic peak on the DTA curve [DTA<sub>max</sub> = 385 °C for **Fe-hepH-Ni**, DTA<sub>max</sub> = 336 °C for **Ni-hepH-Ni**] is associated with the decomposition and burning of the cyanide ligands.

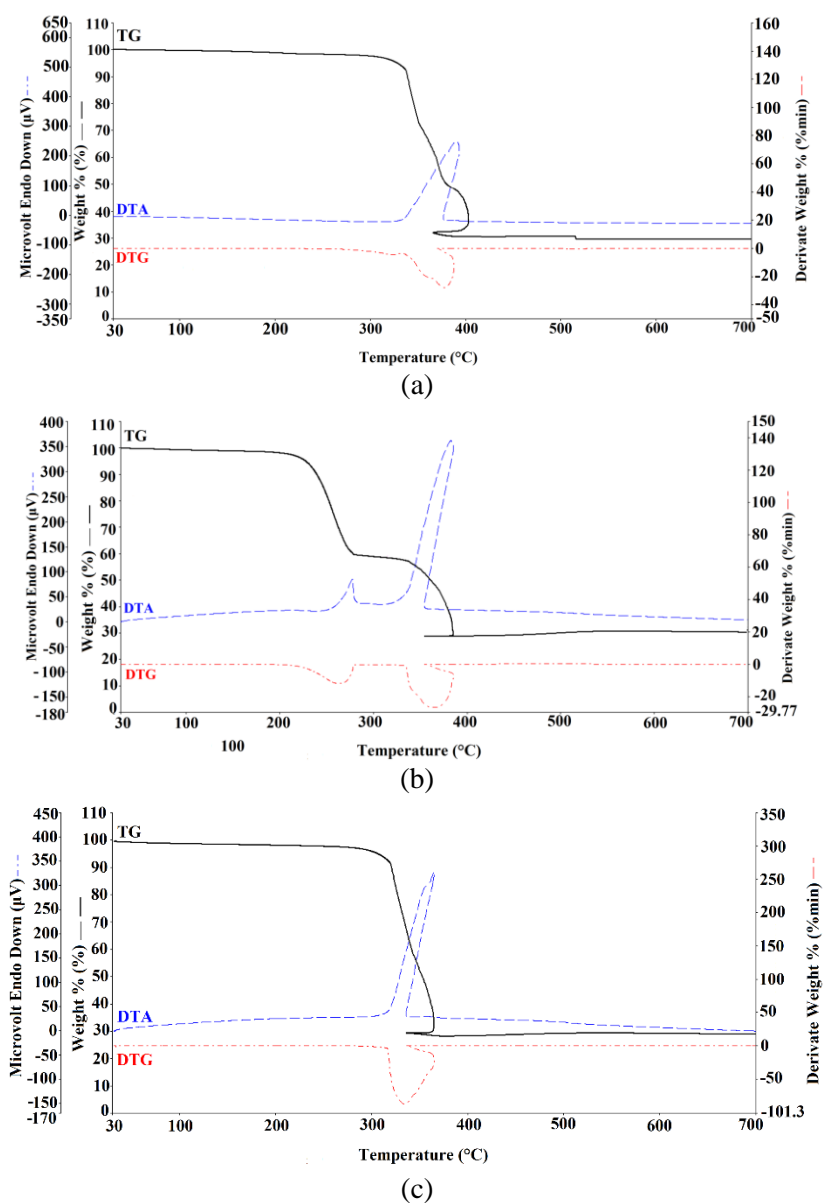


**Figure 4.** The TG, DTG and DTA curves of Fe-hepH-Ni (a), Co-hepH-Ni (b) and Ni-hepH-Ni(c)

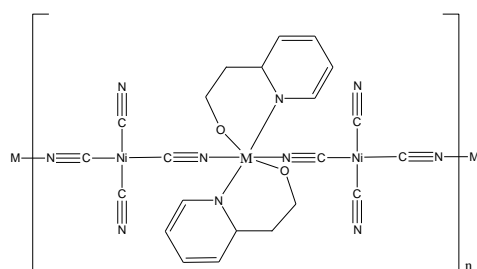


**Figure 5.** The molecular structures of the complexes

### 3.4 Conductivity

The conductivities of the complexes are measured by the standard four-point probe method in the dc plane. In semiconductor materials, conduction mechanisms depend on several parameters such as the degree of crystallinity, thermal excitation, impurities, lattice defects, non-stoichiometry and temperature. Bridging-cyanide ligands also provide reasonable low energy gaps. For example, one solubilized 2,3-naphthalocyaninatocobalt(II) shish kebab polymer with bridging cyanide ligand has an inherent conductivity of almost  $10^{-1}$  S/cm [29]. The electrical conductivities of the complexes are founded as  $0.34 \mu \text{ Scm}^{-1}$  for **Fe-hepH-Ni**,  $0.58 \mu \text{ Scm}^{-1}$  for **Co-hepH-Ni** and at  $3.5 \mu \text{ Scm}^{-1}$  for **Ni-hepH-Ni**. According to these results, the complexes show a weak semiconductive behavior at room temperature. The similar conductivity measurements have been reported previously;  $1.10^{-10} \text{ Scm}^{-1}$  for **PcFe(py)CN** and  $3.10^{-12} \text{ Scm}^{-1}$  for **PcCo(py)CN** [30],  $2.596 \times 10^{-8} \Omega^{-1} \text{ cm}^{-1}$  for **Mn-Ni-etim**,  $2.047 \times 10^{-8} \Omega^{-1} \text{ cm}^{-1}$  for **Fe-Ni-etim**,  $1.137 \times 10^{-7} \Omega^{-1} \text{ cm}^{-1}$  for **Co-Ni-etim** and  $1.923 \times 10^{-9} \Omega^{-1} \text{ cm}^{-1}$  for **Ni-Ni-etim** [31].

### 3.5 Magnetic Properties

The magnetic susceptibility of the complexes was determined by Evans Method. The effective magnetic moments represented in Bohr magnetons (BM) of the complexes are given in Table 1, together with elemental analysis results. The Ni(II) atom is in a square-planar environment (tetracyanonickelate(II) is low spin ( $S=0$ ), diamagnetic and only the octahedral coordinated metal atoms (M(II)) contribute to the magnetic moments). The magnetic moment values of powdered samples at the room temperature are given as follow; for **Fe-hepH-Ni** complex exhibit magnetic moment values of 4.73 BM which both correspond to four unpaired electrons. **Co-hepH-Ni** complex exhibits magnetic moment values of 3.61 BM which both correspond to three unpaired electrons. **Ni-hepH-Ni** complex exhibits magnetic moment values of 2.92 BM which both correspond to paramagnetic with two unpaired electrons. The complexes are shown a similar measurement to the previously studied  $4.83 \mu_B$  in  $[\text{Co}(\text{TEAH}_2)\text{Ni}(\text{CN})_4] \cdot 2\text{H}_2\text{O}$  [32] (Karadağ and Yılmaz, 2000),  $3.24 \mu_B$  in  $[\text{Ni}(\text{Im})_2[\text{Ni}(\text{CN})_4]]$   $4.59 \mu_B$  in  $\text{Fe}(\text{Im})_2[\text{Ni}(\text{CN})_4]$  [7],  $4.12 \mu_B$  in  $[\text{Co}(\text{etim})\text{Ni}(\text{CN})_4]_n$  [31]. The experimental magnetic moment values are in good agreement with the calculated values.

## 4. CONCLUSIONS

Three new cyanide-bridged heteronuclear polymeric complexes,  $[\text{M}(\text{hepH})_2\text{Ni}(\mu\text{-CN})_2(\text{CN})_2]$  (M(II) = Fe, Co and Ni; hepH=2-pyridineethanol), were synthesized and characterized by vibrational (FT-IR and Raman) spectroscopy, thermal and elemental analysis techniques. FT-IR and Raman spectral analyses indicate that the complexes are isostructural with together. Moreover, FT-IR spectra of the complexes were pointed out the existence of terminal and bridged cyanide ligands in the complexes. The complexes showed a conductivity of  $10^{-8}$  S/cm at room temperature. Furthermore, the complexes are shown the paramagnetic behavior.

## ACKNOWLEDGEMENT

This paper is dedicated to Prof. Dr. Ziya KANTARCI, who died on January, 2012.

## REFERENCES

- [1] Batten SR, Neville SM, Turner DR. Coordination polymers: design, analysis and application. Royal Society of Chemistry: Cambridge, UK, 2009.
- [2] Janiak C. Engineering coordination polymers towards applications. Dalton Trans 2003; 14: 2781-2804.

- [3] Korkmaz ŞA, Karadağ A, Yerli Y, Soylu MS. Synthesis and characterization of new heterometallic cyanido complexes based on  $[\text{Co}(\text{CN})_6]^{3-}$  building blocks: crystal structure of  $[\text{Cu}_2(\text{N-bishydeten})_2\text{Co}(\text{CN})_6] \cdot 3\text{H}_2\text{O}$  having a strong antiferromagnetic exchange. *New J Chem*. 2014; 38; 5402-5410.
- [4] Černák J, Orendáč M, Potočňák I, Chomič J, Orendáčová A, Skoršepa J, Feher A. Cyanocomplexes with one-dimensional structures: preparations, crystal structures and magnetic properties. *Coord Chem Rev* 2002; 224: 51-66.
- [5] Kajňáková M, Černák J, Kavečanský V, Gérard F, Papageorgiou T, Orendáč M, Orendáčová A, Feher A. Magneto-structural correlations. Rietveld refinement of the three-dimensional crystal structure of  $\text{Mn}(\text{en})\text{Ni}(\text{CN})_4$  (en= ethylenediamine) and magnetic interactions through the  $[\text{Ni}(\text{CN})_4]^{2-}$  anion. *Solid State Sci* 2006; 8: 203-207.
- [6] Ouahab L, Setifi F, Golhen S, Imakubo T, Lescouëzec R, Lloret F, Julve M, Świetlik R. Charge transfer salts containing a paramagnetic cyano-complex and iodine substituted organic donor involving  $-\text{I}_{(\text{donor})} \cdots \text{N}_{(\text{anion})}^-$  interactions. *C R Chim* 2005; 8; 1286-1297.
- [7] González M, Lemus-Santana A, Rodríguez-Hernández J, Knobel M, Reguera E.  $\pi \cdots \pi$  interactions and magnetic properties in a series of hybrid inorganic–organic crystals. *J Solid State Chem* 2013; 197: 317-322.
- [8] Hoskins B, Robson R. Design and construction of a new class of scaffolding-like materials comprising infinite polymeric frameworks of 3D-linked molecular rods. A reappraisal of the zinc cyanide and cadmium cyanide structures and the synthesis and structure of the diamond-related frameworks  $[\text{N}(\text{CH}_3)_4][\text{Cu}^{\text{I}}\text{Zn}^{\text{II}}(\text{CN})_4]$  and  $\text{Cu}^{\text{I}}[4, 4', 4'', 4''']\text{-tetracyanotetraphenylmethane}[\text{BF}_4 \cdot x\text{C}_6\text{H}_5\text{NO}_2]$ . *J Am Chem Soc* 1990; 112: 1546-1554.
- [9] Herebian D, Wieghardt KE, Neese F. Analysis and Interpretation of Metal-Radical Coupling in a Series of Square Planar Nickel Complexes: Correlated Ab Initio and Density Functional Investigation of  $[\text{Ni}(\text{L}^{\text{ISQ}})_2](\text{L}^{\text{ISQ}} = 3, 5\text{-di-tert-butyl-o-diiminobenzosemiquinonate (1-))$ . *J Am Chem Soc* 2003; 125: 10997-11005.
- [10] Lescouëzec R, Lloret F, Julve M, Vaissermann J, Verdaguer M.  $[\text{Fe}(\text{bipy})(\text{CN})_4]^-$  as a versatile building block for the design of heterometallic systems: synthesis, crystal structure, and magnetic properties of  $\text{PPh}_4[\text{Fe}^{\text{III}}(\text{bipy})(\text{CN})_4] \cdot \text{H}_2\text{O}$ ,  $[\{\text{Fe}^{\text{III}}(\text{bipy})(\text{CN})_4\}_2\text{M}^{\text{II}}(\text{H}_2\text{O})_4] \cdot 4\text{H}_2\text{O}$ , and  $[\{\text{Fe}^{\text{III}}(\text{bipy})(\text{CN})_4\}_2\text{Zn}^{\text{II}}] \cdot 2\text{H}_2\text{O}$  [bipy = 2, 2'-Bipyridine; M= Mn and Zn]. *Inorg Chem* 2002; 41: 818-826.
- [11] Bullinger JC, Moore CE, Eichhorn DM. Recent advances in cyanoscorpionate chemistry: complexes with Co(II), Mn(II), and Ni(II)(cyclam). *Proceedings of the 4th Annual GRASP Symposium*; 25 April 2008; Wichita, KS: Wichita State University, p.23-24
- [12] Sayın E, Kürkçüoğlu GS, Yeşilel OZ, Hökelek T. C-H $\cdots$ Pd interactions: One dimensional heteropolynuclear complexes. *Spectrochim Acta Part A* 2014; 132: 803-814.
- [13] Sayın E, Kürkçüoğlu GS, Yeşilel OZ, Hökelek T. Syntheses and characterizations of tetracyanoplatinate(II) complexes with 2-pyridineethanol. *J Coord Chem* 2015; 68: 2271-2285.
- [14] Kürkçüoğlu GS, Sayın E, Gör K, Arslan T, Büyükgüngör O. C-H $\cdots$ Ni Interactions and Cyano-Bridged Heteronuclear Polymeric Complexes Studied by Vibrational Spectroscopy and Quantum Chemistry Calculations. *Vib Spectrosc* 2014; 71: 105-117.
- [15] Aggarwal K, Khurana JM. X-ray diffraction, spectroscopic characterization and quantum chemical calculations by DFT and HF of novel 2-hydroxy-12-(4-hydroxyphenyl)-9,9-dimethyl-9,10-dihydro-8H-benzo[a]xanthen-11(1 H)-one. *J Mol Struct* 2015;1079: 21-34.
- [16] Michalska D, Bienko D, Abkowicz-Bienko A, Latajka Z. Density functional, Hartree-Fock, and MP2 studies on the vibrational spectrum of phenol. *J Phys Chem* 1996; 100: 17786-17790.

- [17] Arjunan V, Balamourougane PS, Govindaraja ST, Mohan S. A comparative study on vibrational, conformational and electronic structure of 2-(hydroxymethyl)pyridine and 3-(hydroxymethyl)pyridine. *J. Mol. Struct* 2012; 1018: 156-170.
- [18] Socrates G, *Infrared and Raman characteristic group frequencies: tables and charts*. 3rd ed. John Wiley & Sons, Chichester, England, 2004.
- [19] Varsányi G, *Assignments for vibrational spectra of seven hundred benzene derivatives*. 1. Halsted Press, Wiley-Interscience: New York, 1974.
- [20] Arjunan V, Mohan S. Fourier transform infrared and FT-Raman spectra, assignment, ab initio, DFT and normal co-ordinate analysis of 2-chloro-4-methylaniline and 2-chloro-6-methylaniline. *Spectrochim Acta Part A* 2009; 72: 436-444.
- [21] Arjunan V, Puviarasan N, Mohan S, Fourier transform infrared and Raman spectral investigations of 5-aminoindole. *Spectrochim Acta Part A* 2006; 64: 233-239.
- [22] Nakamoto K. *Infrared and Raman spectra of inorganic and coordination compounds*. Part B., Applications in coordination, organometallic, and bioinorganic chemistry. 6th ed. John Wiley&Sons, Hoboken, New Jersey, 2009.
- [23] McCullough R, Jones L, Crosby G. An analysis of the vibrational spectrum of the tetracyanonickelate(II) ion in a crystal lattice. *Spectrochim Acta* 1960; 16: 929-944.
- [24] Nakamoto K. *Infrared and Raman spectra of inorganic and coordination compounds*. 3rd ed. Wiley, New York, 1978.
- [25] Bignozzi CA, Argazzi R, Schoonover JR, Gordon KC, Dyer RB, Scandola F. Electronic coupling in cyano-bridged ruthenium polypyridine complexes and role of electronic effects on cyanide stretching frequencies. *Inorg Chem* 1992; 31: 5260-5267.
- [26] Kubas GJ, Jones, LH. Potential constants of the tetracyanide ions of nickel, palladium, and platinum. *Inorg Chem* 1974; 13: 2816-2819.
- [27] Vitoria P, Beitia JI, Gutiérrez-Zorrilla JM, Sáiz ER, Luque A, Insausti M, Blanco JJ. Tetracyanometalates of Ni, Pd, and Pt with cyclic diquaternary cations of 2, 2'-bipyridine and 1, 10-phenanthroline. A vibrational, crystallographic, and theoretical study of intermolecular weak interactions. *Inorg Chem* 2002; 41: 4396-4404.
- [28] Parlak C. FT-IR and Raman spectroscopic analysis of some Hofmann type complexes. *Spectrochim Acta Part A* 2012; 99: 12-17.
- [29] Hanack M, Polley R, Knecht S, Schlick U. Reaction of cyanogen with cobalt phthalocyanines. *Inorg Chem* 1995; 34: 3621-3624.
- [30] Hanack M, Hirsch A, Lange A, Rein M, Renz G, Vermehren P. Bridged macrocyclic transition metal complexes, a new type of semiconducting materials. *J Mater Res* 1991; 6: 385-392.
- [31] Kürkçüoğlu GS, Kiraz FÇ, Sayın E. Vibrational spectra, powder X-ray diffractions and physical properties of cyanide complexes with 1-ethylimidazole. *Spectrochim Acta Part A* 2015; 149: 8-16.
- [32] Karadağ A, Yılmaz VT. Preparation and Infrared Spectroscopic Examination of Hofmann-Type Di- and Triethanolamine Complexes. *Synth React Inorg Met -Org Chem* 2000; 30: 359-368.